

# Adhesion, lubrication and wear on the atomic scale

James B. Adams,<sup>1\*</sup> Louis G. Hector Jr,<sup>2</sup> Donald J. Siegel,<sup>3</sup> Hualiang Yu<sup>4</sup> and Jun Zhong<sup>1</sup>

<sup>1</sup> Department of Chemical and Materials Engineering, Arizona State University, Tempe, AZ 85287-6006, USA

<sup>2</sup> Alcoa Technical Center, Alcoa Center, PA 15069-0001, USA

<sup>3</sup> Department of Physics, University of Illinois at Urbana-Champaign, 1110 West Green St, Urbana, IL 61801, USA

<sup>4</sup> Science and Engineering of Materials Program, Arizona State University, Tempe, AZ 85287-1704, USA

Received 8 November 2000; Revised 12 December 2000; Accepted 2 January 2001

This paper reviews three important aspects of tribology (adhesion, lubrication and wear) on the atomic scale with a focus on our work on aluminum surfaces. Adhesion is critical to the success of many applications but there is no simple analytical model available to predict adhesion between different materials, so we discuss the use of electronic structure methods to investigate adhesion between Al and various ceramics to determine the factors that control adhesion. Lubricants used to control friction usually include 'boundary additives' to bind the lubricant more strongly to the surface, so that higher stresses can be employed and wear can be reduced. Little is known about how boundary additives bond to Al surfaces, so we used electronic structure methods to investigate that phenomenon. Regarding wear, we review the literature on molecular dynamics simulations to investigate nanoindentation and wear. We discuss our molecular dynamics simulations of nanoindentation and asperity–asperity shear and the effect of temperature, loading rate, interaction strength and geometry. Copyright © 2001 John Wiley & Sons, Ltd.

**KEYWORDS:** adhesion; lubrication; wear; molecular dynamics

## INTRODUCTION

Adhesion, lubrication and wear are processes that affect many industries, including metal forming, aerospace, automotive and microelectronics. Adhesion is critical to the success of many applications, from automotive tires (the infamous Firestone tire problem is largely due to debonding of the rubber from the steel wires) to semiconductor circuits (each deposited layer must adhere strongly to the layer beneath it to survive thermal stresses). Similarly, wear has a tremendous effect on the US industry, with wear problems estimated to cost US\$8 billion annually, because wear determines the lifetime of many parts, from automotive engines components to airplane brakes. On the positive side, many machining operations rely upon wear processes (from oil drilling to polishing an Si wafer) and optimization of these processes is critical to commercial success. There is an increasing interest in dry machining, because the oils used during machining are easily evaporated due to frictional heating, and there is a rapidly rising concern about the impact of such vapors on the long-term health of machine operators. Thus, it is clear that a better understanding of adhesion, lubrication and wear will have a positive impact on many industries and help lead to 'greener' manufacturing. Unfortunately the field remains dominated by Edisonian approaches yielding short-term solutions; we believe that

there is a great need for a fundamental, atomic-scale study of the critical mechanisms and processes involved in adhesion, lubrication and wear.

One example is the processing of aluminum alloys, which is relevant also to the processing of many other metallic alloys. Aluminum alloy products are manufactured through a series of processing steps that begin with casting an aluminum ingot. In order to reduce the thickness of the ingot, it is passed through a series of rolling operations under high loads at speeds up to 4500 feet min<sup>-1</sup> (Fig. 1). Lubricants are used to control interface heating due to friction and plastic deformation. They contain additives that react with the aluminum to form molecularly thin 'boundary' layers that mitigate adhesion and adhesive transfer. Because the surface area approximately doubles after each rolling step, new surfaces of non-oxidized Al are being formed continuously and can come into contact with the roller. If critical stresses and/or rates are exceeded, wear rates can increase by 100× or more as Al is torn from the sheet and coats the roller, resulting in a process instability and damage to the part. If one could design an improved lubricant and combine it with an appropriate coating system that is 'tuned' to key process and product attributes, then Al parts with superior surface quality could be formed at higher strain rates with processing steps.

Another example involving materials performance is the use of aluminum parts in engine blocks. General Motors and other automotive companies are converting cast-iron engine blocks to aluminum because aluminum engine blocks can weigh 40–50% less than a comparable cast-iron block. However, the poor wear resistance and low seizure loads of

\*Correspondence to: J. B. Adams, Department of Chemical and Materials Engineering, Arizona State University, Tempe, AZ 85287-6006, USA. E-mail: jim.adams@asu.edu  
Contract/grant sponsor: National Science Foundation;  
Contract/grant number: DMR 9619353.

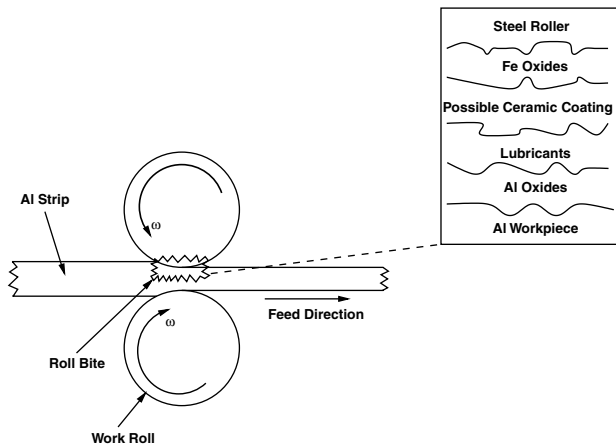


**Figure 1.** The strip rolling process and a realistic toolpiece/workpiece interface.

the 319 and 356 Al–Si-based alloys are a major drawback for their use in engine applications. Finding a lubricant and/or coating system to reduce friction and wear would enable increased engine power density, durability and performance.

The three general areas that we will review in this paper are adhesion, lubrication and wear, with a focus on our group's work on aluminum:

- (1) Adhesion: there is no simple analytical model to predict adhesion between different materials, so we discuss the use of electronic structure methods to investigate adhesion between Al and various ceramics, to determine the factors that control adhesion.
- (2) Lubrication: high stresses during forming can result in lubricant being forced out, so that the toolpiece and the Al workpiece come into contact. Lubricant boundary additives are added to bind the lubricant more strongly to the surface, so that higher stresses can be employed and wear can be reduced. Little is known about how boundary additives bond to Al surfaces, so we decided to use electronic structure methods to investigate how lubricant additives bind to Al.
- (3) Wear: wear can occur in several ways during Al processing, including especially adhesive wear (the Al bonds with the steel) and abrasive wear (hard surface asperities in the tool plow through the soft Al). Relatively little is understood about the atomic-scale mechanisms that occur during wear, so we decided to use molecular dynamics simulations to investigate several wear mechanisms.

In the following sections we will review the literature in each area, present some examples of our own work and discuss what we think are some of the outstanding challenges in the field. Although in our work we focus on aluminum, we believe that our results are relevant to many materials systems in which adhesion, lubrication and wear occur.

## ADHESION AT METAL/CERAMIC INTERFACES

### Review of the literature

The ideal work of adhesion,  $W_{ad}$ ,<sup>1</sup> is defined as the energy needed for reversible separation on an interface into two free

surfaces, neglecting deformation. Although these dissipative processes dictate that the energy needed in an actual cleavage experiment always will be greater than the ideal work of adhesion (due to plastic deformation), the larger  $W_{ad}$ , the more work must be done to cleave the interface. Formally,  $W_{ad}$  can be defined in terms of either the surface and interfacial energies (relative to the respective bulk materials) or the difference in total energy between the interface and its isolated slabs

$$W_{ad} = \sigma_{1v} + \sigma_{2v} - \sigma_{12} = (E_1^{tot} + E_2^{tot} - E_{12}^{tot})/2A$$

Here,  $\sigma_{iv}$  is the surface energy of slab  $i$ ,  $\sigma_{12}$  is the interface energy,  $E_i^{tot}$  is the total energy of slab  $i$ ,  $E_{12}^{tot}$  is the total energy of the interface system and  $A$  is the interface area, assuming a system with two identical interfaces.

To date, the available analytical models for predicting  $W_{ad}$  are limited to liquid-metal/oxide interfaces and rely on simple empirical correlations that incorporate either the free energy of formation of the oxide of the liquid metal or the enthalpies of mixing of the respective oxide elements in the metal.<sup>2–8</sup> Unfortunately, many of these models are not applicable to systems in which the ceramic is not an oxide, do not address solid-on-solid interfaces, can be difficult to parameterize, and generally provide only qualitative information about trends in adhesion. Furthermore, their range of applicability—even within the class of metal/oxide interfaces—is questionable because many have been applied only to systems using  $\alpha$ -Al<sub>2</sub>O<sub>3</sub> (alumina) as the oxide.

In light of the shortcomings of the above models, it should come as no surprise that the last 5 years have seen rapid growth in the number of first-principles studies of metal/ceramic adhesion based in density functional theory (DFT).<sup>9,10</sup> Not only are these methods highly accurate, but they can provide invaluable information regarding the detailed atomic and electronic structure of the interface. (For a thorough review of this work up to 1995, see Ref. 1.) Whereas most investigations prior to 1995 focused almost exclusively on oxide ceramics and on a small number of model systems, there has been a move recently to study interfaces of more technological relevance<sup>11–20</sup> while introducing more realistic models that incorporate interfacial defects and impurities,<sup>21–23</sup> more diverse geometries<sup>24</sup> and the effects of the environment.<sup>25</sup> Nevertheless, only a very small number of systems have been investigated with these methods, with most work still focused on oxide/metal interfaces. Unfortunately, much less is known about interfaces involving non-oxide ceramics such as carbides and nitrides, which are commonly used as tribological coatings.

### Previous work

#### *Density functional studies of the Al/alumina interface*

In our previous work we conducted a thorough *ab initio* study (using DFT as implemented in the VASP<sup>26</sup> code) of the Al(111)/ $\alpha$ -Al<sub>2</sub>O<sub>3</sub> interface.<sup>27</sup> This interface is important because it serves as a model for the typical oxide that forms on Al and is one of the few metal/ceramic systems for which the adhesion energy has been measured experimentally. Our calculations involved placing bulk-like slabs into contact and taking into account the effects of stacking sequence, oxide

termination (Al or O) and full atomic relaxations. In all, we considered six different candidate interface structures. We found that, regardless of oxide termination, the optimal interface geometry was obtained for the stacking sequence that placed the metal atoms above the oxygen hole sites in the alumina (henceforth referred to as the 'fcc' stacking sequence). An atomic geometry optimization resulted in substantial atomic displacements in the metal near the interface, wherein some atoms were pulled towards the oxide and assumed positions that normally would be occupied by the  $\text{Al}^{3+}$  cations in the bulk crystal (see Plate 1). The subsumed atoms are arranged such that they effectively terminate the oxide with a bilayer of Al, independent of its initial termination. Based on their positions and electronic structure, it seems more natural to consider these atoms as belonging to the oxide slab rather than to the metal, with the location of the metal/ceramic interface shifted away from the oxide. These atomic distortions also opened up small charge density voids within the near-interface region of the metal, suggesting possible fracture points near the interface when loaded in tension.

Two methods were used to estimate the ideal work of adhesion. First, we performed a series of total energy vs. interfacial separation calculations using unrelaxed slabs and fitted the data to the universal binding energy relation (UBER)<sup>28</sup> to obtain the optimal interfacial separation and adhesion energy. These geometries then were used as starting points for a determination of the relaxed interfacial structures and their corresponding adhesion energies. In allowing for atomic relaxations, we found that both the magnitude and rank ordering of the adhesion energies for the different stacking sequences changed relative to the unrelaxed results (see Plate 1 for a comparison of unrelaxed vs. relaxed geometries). This is important because some previous studies relied on UBER curves without accounting for atomic relaxations. Our results show that approach to be incorrect, both quantitatively and qualitatively, for this system that undergoes large relaxations. We find that for the Al-terminated interface the calculated adhesion energies of  $1.36 \text{ J m}^{-2}$  (LDA) and  $1.06 \text{ J m}^{-2}$  (GGA) for the relaxed fcc-Al interface are in good agreement with the experimental value of  $1.13 \text{ J m}^{-2}$ .<sup>29</sup> (The experimental value is probably slightly low due to some sub-monolayer water contamination, but even a slightly higher value is still consistent with our calculations.) For the fcc O-terminated interface these values are about an order of magnitude larger:  $10.7$  and  $9.73 \text{ J m}^{-2}$ , respectively. Tabulated adhesion energies and equilibrium interfacial distances for all six candidate structures can be found in Table 1.

There is still considerable debate as to what the dominant bonding mechanisms are at metal/ceramic interfaces. To clarify this issue, we applied five techniques to thoroughly analyze the interfacial bonding, including partial densities of states (DOS), electron localization function (ELF),<sup>30</sup> charge density, Mayer bond order<sup>31</sup> and Mulliken populations.<sup>32</sup> Our primary finding is that the interfacial Al–O bonds in both systems are very similar to the cation–anion bonds found in bulk alumina, and therefore are mainly ionic with a smaller degree of covalency. In the O-terminated

**Table 1.** Relaxed and unrelaxed values for ideal work of separation ( $W_{\text{ad}}$ ), and minimum interfacial distance ( $d_0$ ), for the Al/alumina interface system. The units are  $\text{J/m}^2$  and  $\text{\AA}$ , respectively

Stacking	Termination	Unrelaxed (UBER)		Relaxed		
		$d_0$	$W_{\text{ad}}$ (LDA)	$d_0$	$W_{\text{ad}}$ (LDA)	$W_{\text{ad}}$ (GGA)
fcc	Al	2.55	1.14	0.70	1.36	1.06
hcp	Al	2.26	1.33	2.57	0.69	0.41
ot	Al	2.09	1.55	1.62	1.18	0.84
fcc	O	1.45	9.11	0.86	10.7	9.73
hcp	O	1.38	9.56	1.06	10.3	9.11
ot	O	1.71	9.43	2.00	9.90	8.75
Experiment <sup>29</sup>					1.13	

interface this ionic interaction (via charge transfer from metal to oxide) is the dominant bonding mechanism and it is responsible for the larger adhesion energies. However, for the fcc/Al interface, our ELF (see Plate 1) and bond order analysis indicate that there is some additional covalent bonding between the oxide's Al monolayer and an interfacial metal atom. By analyzing Mulliken charges we determined that there is twice as much charge transfer to the oxide in the O-terminated interface relative to the Al termination, and that the charge state of the subsumed metal atoms is consistent with the cation charges in the bulk. The bond orders and Mulliken populations in the oxide generally are unchanged by the presence of the interface, suggesting that most of its bonding requirements are satisfied by oxidizing the subsumed atoms. On the other hand, there is a significant reduction in metallic bonding in the Al slab near the interface, with a corresponding increase in more directional, covalent-type back-bonds. In conclusion, we found that bonding at the Al/ $\alpha$ - $\text{Al}_2\text{O}_3$  interface can range from mostly ionic (for the oxide termination) to a combination of ionic and covalent (for the Al termination).

### Density functional study of the Al/WC interface

In addition to our study of the Al/ $\alpha$ - $\text{Al}_2\text{O}_3$  system, we have also completed calculations on the Al(111)/WC(0001) interface (details available from the author upon request). Tungsten carbide (WC) is an important wear-resistant coating material in Al manufacturing, the automotive industry and in other tribological applications such as dry machining. To our knowledge, these calculations are the first to examine this interface.

As we did for the Al/alumina system, we applied both the UBER and full relaxation methods for estimating the adhesion energy for several candidate interface structures. (Because the (0001) plane of WC is a polar surface (it can be terminated by a monolayer of either W or C), we investigated both possible terminations. For each termination we also considered several different stacking sequences for a total of 11 candidate interface geometries. We found that for both terminations the strongest adhesion occurs when the Al interface atom is placed in the hcp site relative to the wc(0001) surface, with the close packed directions

matched across the interface:  $[11\bar{2}0]_{\text{WC}}||[1\bar{1}0]_{\text{Al}}$ . Furthermore, the C-terminated interface is the strongest overall, with a work of adhesion of  $6.2 \text{ J m}^{-2}$ . This should be compared with the W-terminated adhesion energy of  $4.0 \text{ J m}^{-2}$ , which is still relatively large. These calculations suggest that WC is not an optimal coating material for reducing adhesion in Al manufacturing processes, because the interfacial bond is likely to be stronger than the cohesive strength of the Al. To investigate this scenario further, we followed up with a series of virtual separation simulations in which we calculated the work of separation of the optimal C-terminated WC/Al interface at several cleavage points. Whereas  $6.2 \text{ J m}^{-2}$  of work was necessary to separate the interface at the Al/WC plane, cleavage within the Al slab (with the first monolayer of Al transferred to the WC) required only  $2.5 \text{ J m}^{-2}$ , which is less than half that needed to separate the interface without adhesive transfer. Cleavage one layer deeper into the Al (two monolayers transferred to the WC) required  $2.9 \text{ J m}^{-2}$ . By comparison, cleavage within the WC was very unfavorable, requiring  $>11 \text{ J m}^{-2}$ . In conclusion, we found that WC binds strongly to Al and hence is not an ideal coating material for tools used to form Al parts.

## LUBRICANT BOUNDARY ADDITIVES

### Review of the literature

Lubricant formulations used to control friction and wear in bulk metal-forming processes such as rolling, extrusion and forging, and in mechanical contacts such as those found in drive train systems and engine components, contain long-chain hydrocarbon molecules often referred to as boundary additives. These molecules are functionalized at one end with ionic species that are intended to react with a metallic (or oxide) surface, leaving a dangling hydrocarbon chain that protrudes from the surface. Extreme pressures often lead to changes in the rheological properties of the films. For example, it is now well established that at interfacial separations of the order of a few molecular chain lengths the viscosities increase by several orders of magnitude.<sup>33,34</sup> A comprehensive review of previous work on the computer simulation of molecular-scale lubrication can be found in Ref. 35. At present, most of the work in this area has considered additive and/or base oil behavior in the absence of substrate deformation for non-ferrous surfaces such as carbon and gold. The mechanisms of boundary film lubrication for metallic and oxide surfaces undergoing abrasive and adhesive wear are currently unknown and little is known about the chemical reactions that result in bonding of the additives to the surface.

Existing literature on lubricant additive simulation for engine components deals mostly with additive interactions with iron oxide surfaces. For example, Jiang *et al.*<sup>36</sup> modeled dithiophosphate performance as a wear inhibitor for iron oxide surfaces. Simulation of thermal stability and friction of confined wear inhibitor was considered by Cagin *et al.*<sup>37</sup> Zhou *et al.*<sup>38</sup> investigated the performance of both dithiophosphate and dithiocarbamate as engine wear inhibitors. An extensive discussion of boundary additive chemistries is found in Shey.<sup>39</sup> There is no extreme pressure additive

currently available for aluminum engine components and no design criteria with which additive functional groups could be 'tuned' to the material and process-specific needs of aluminum engine components.

Several studies have provided hints as to how boundary additives can react with and bond to the surfaces of aluminum metal and aluminum oxide. For example, Rogers *et al.*<sup>40</sup> studied the decomposition of methanol on aluminum using spectroscopic methods. They found that above 500 K the methanol decomposes, leading to oxidation of the aluminum surface and the formation of methane. At present, the mechanism of ester decomposition on aluminum is unknown.<sup>41,42</sup> Recent spectroscopic work by Hooper *et al.*<sup>43</sup> on an idealized system revealed that vapor-deposited aluminum atoms will react with the  $-\text{CO}_2\text{CH}_3$  group in a self-assembled monolayer (SAM) of  $\text{HS}(\text{CH}_2)_{15}\text{CO}_2\text{CH}_3$  but will not react with the  $\text{CH}_3$  groups in a SAM of  $\text{HS}(\text{CH}_2)_{15}\text{CH}_3$ . Underhill and Timsit<sup>44</sup> investigated the decomposition of short-chain alcohols and carboxylic acids on a clean aluminum surface across a range of temperatures. They found that, when heated, both the alcohol and carboxylic acid molecules dissociate between 100 °C and 150 °C. Above 150 °C, the oxygen is liberated completely from the additive functional group. This leads to oxidation of the aluminum surface and direct attachment of the alkyl chain to the surface through the functional carbon atom. However, the reaction process has not been investigated theoretically. In addition, none of these studies addressed the molecular-scale lubrication mechanisms associated with adhesive and abrasive wear of aluminum surfaces and how these are linked ultimately to macroscopic behavior.

### Density functional studies of lubricant boundary additives

In our current project, we have begun some of the first theoretical studies of the interactions of several idealized boundary additives with Al surfaces<sup>45</sup> (details available from the author upon request). During a bulk metal-forming process, the surface area of the plastically deforming workpiece increases due to volume constancy of plastic deformation. The subsequent elongation of the workpiece breaks up the native surface oxide, which is 3–6 nm thick, and fresh nascent Al is exposed. This clean Al surface is suspected to be the major cause of adhesive wear because it is highly reactive with the oxide surfaces of typical steel tools, so it is especially important that boundary additives form protective layers on the fresh Al. (The thermit reaction,  $\text{Al} + \text{Fe}_2\text{O}_3 \rightarrow \text{Al}_2\text{O}_3 + \text{Fe}$ , is so exothermic that it will melt the  $\text{Al}_2\text{O}_3$  and boil the Fe.)

Based upon a methodology suggested by G. Kresse, we selected three different functional groups commonly used in Al processing,<sup>39</sup> *viz.* alcohol, carboxylic acid and ester, and investigated their decomposition on Al(111) at 0 K. The chain lengths were shortened on these molecules because the tails are not involved in reaction with the surface. We therefore focused directly on the functional group behavior because it is the strength of the bond between the chains and the surface that establishes the basis for the formation of a durable boundary film. Using the VASP code,<sup>26</sup> we first investigated the adhesion energy of each

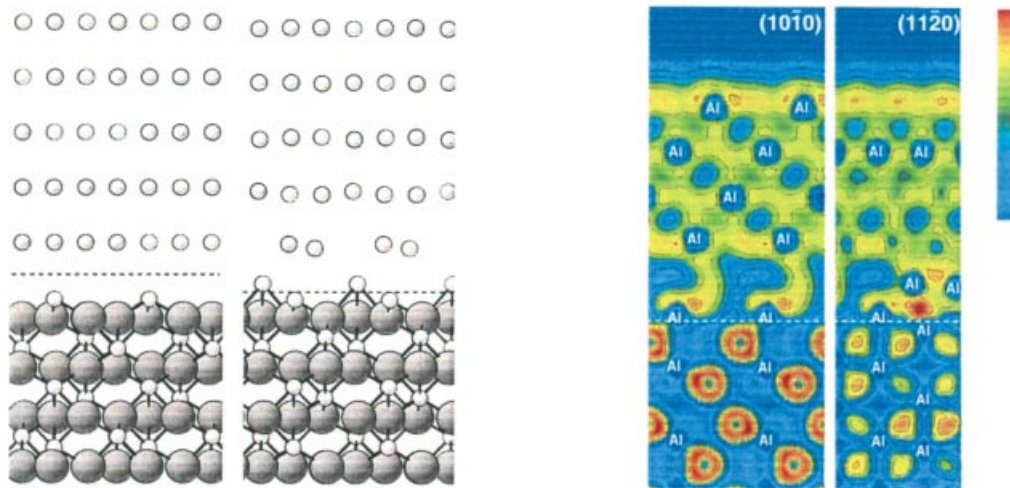


**Plate 1.** (a) (*Left*) The lowest energy geometry of the fcc-Al interface as predicted by UBER calculations; (*right*) the final relaxed structure. Small spheres represent Al atoms; large spheres represent O atoms. The direction of view is along  $[1\bar{2}10]$ . (The lower portion of the structure has been omitted for clarity.) (b) Two slices through the electron localization function for the fcc-Al interface taken along the  $(10\bar{1}0)$  and  $(11\bar{2}0)$  planes, showing four of the hexagonal close-packed oxygen layers in the oxide (*bottom*) and all five atomic layers from one of the Al slabs (*top*).

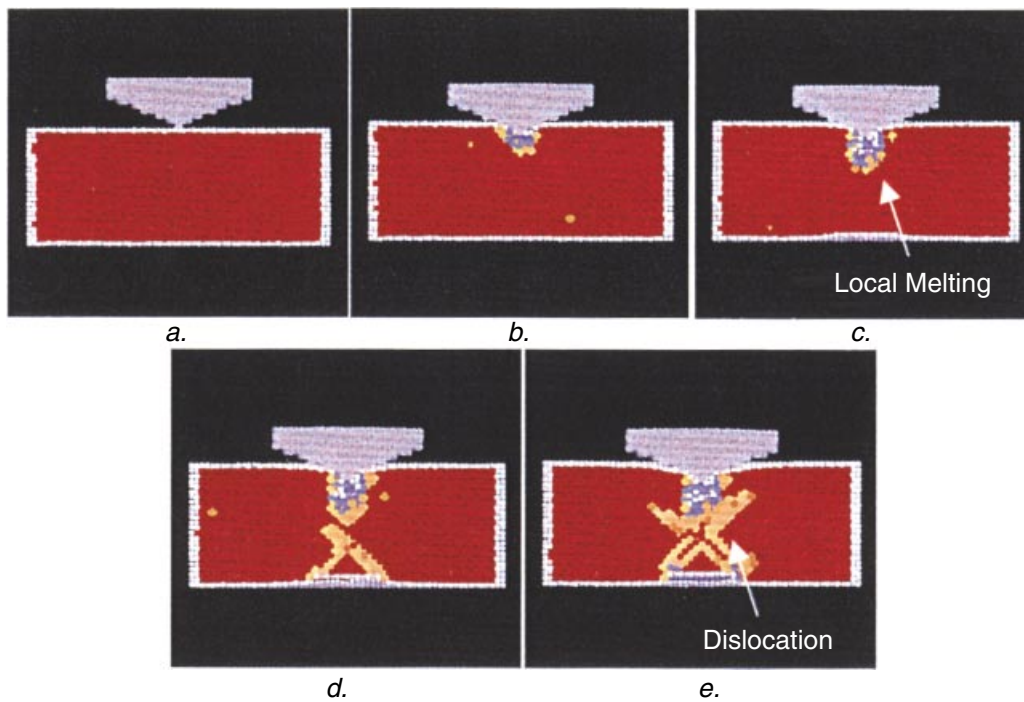


**Plate 2.** Molecular dynamics simulations of nanoindentation into Al at 300 K, showing local melting near the tip, followed by dislocation, nucleation and motion on  $(111)$  planes (dislocations visualized as line of orange atoms).

molecule to several sites on the surface (physisorption). Then we investigated the thermodynamics of a series of decomposition pathways following the experimental findings of Underhill and Timsit.<sup>44</sup> For the alcohol, we found that it was energetically favorable for it to decompose by first losing a hydrogen and then an oxygen, finally resulting in the carbon backbone bonding directly to the Al surface with a net reaction enthalpy of 42 kcal mol<sup>-1</sup>. We considered a similar pathway for the acid and found a much larger net reaction enthalpy of 83 kcal mol<sup>-1</sup>.

We also investigated an ester group because it was debated whether or not it would decompose on Al(111). We began by examining two possible ways in which it can physisorb to the surface—through its carbonyl group and through both its carbonyl and ester group—and found that the latter was favorable by 0.2 eV. We investigated three possible decomposition pathways. We found that decomposition in fact was energetically favorable and we determined which mechanism and decomposition products were the most likely. Altogether, these calculations have provided us with a rich understanding of how several common functional groups on polymer chains can adsorb to aluminum surfaces.

We also carried out a series of *ab initio* molecular dynamics (MD) simulations (details available from the author upon request) to verify that our decomposition pathways were the most favorable and to investigate other possible reaction paths and products. These simulations were carried out at an initial temperature of 300 K, with the molecules approaching the surface at speeds typical of high-speed rolling (around 5000 feet min<sup>-1</sup>). For the alcohol we found that the hydrogen would indeed dissociate, leading to the oxygen binding strongly to the Al(111) surface, which was the first step of our decomposition path. For the acid, we found that one unexpected event was the possible removal of hydrogen from the molecule to the surface, followed by the two oxygens in the molecule chelating an Al and pulling it off the surface. This is very important because it results in a highly polar molecule that will not bond strongly to the surface but rather will raise significantly the viscosity of the lubricant. This phenomenon is referred to as 'soap' formation and is a significant problem during Al processing; this is the first theoretical observation of its occurrence. Thus, our preliminary conclusion is that carboxylic acids and esters can lead to 'soap' formation whereas alcohols will not.

In addition to our work on boundary additives, we investigated also the adhesion of vinyl phosphonic acid (VPA) to a hydroxylated  $\alpha$ -Al<sub>2</sub>O<sub>3</sub> (0001) surface,<sup>46</sup> which is a reasonable model for the passivated native oxide. Vinyl phosphonic acid is of great current interest as a possible anti-corrosion treatment to replace the current chromate coatings that are carcinogenic and will be replaced as soon as a suitable alternative is developed. We investigated in detail how the VPA can bind to the surface. We considered two different molecular conformations and three different sites, and for each we investigated tridentate, bidentate and unidentate reactions, each of which result in the formation of three, two or one water molecules, respectively. We determined that the tridentate structure was preferred, consistent with

spectroscopic studies,<sup>47,48</sup> and we determined that it did bind strongly to the surface (0.5 eV) so is a possible candidate to replace carcinogenic chromate coatings.

Our theoretical work on lubricants was complemented by atomic force microscopy (AFM) single-asperity plowing studies using a diamond indenter as a model asperity.<sup>45</sup> Such studies investigated the plowing of AFM diamond indenters through Al surfaces for dry conditions and for lubricants with a variety of lubricant additives. The addition of acids and esters resulted in more 'softening' of the metal surface than did alcohols or the base oils, consistent with our results that the acids and esters were significantly more reactive with the surface than the alcohols and base oils, although the softening mechanism is not known: it may be due to hydrogen and other decomposition products causing more disruption of the surface structure, so that more wear occurs for the same load. Another possibility rests with what has been referred to as the Rebinder effect, in which surface-active media such as additive molecules move into defects in the surface and subsequently react with the subsurface lattice structure, thereby changing mechanical properties such as hardness and flow strength.<sup>49</sup> This chemomechanical wear mechanism has yet to be investigated at the atomic scale because it may be a prime contributor to the generation of abrasive debris in both metal-forming and mechanical component contacts.

## MOLECULAR DYNAMICS (MD) SIMULATIONS OF NANOINDENTATION/WEAR

### Review of the literature

Indentation experiments have been performed for more than 100 years to measure the hardness of materials. Recently there is a growing interest in measuring the mechanical properties of materials at the micro- and nanometer length scales that are critical to several applications, including tribological coatings, microelectromechanical devices and adhesion of biomolecules and living cells. In the last decade, significant improvements in indentation techniques have been made following the development of AFM. It is possible now to determine, with high precision and accuracy, both the load and displacement of an indenter during indentation experiments in the respective micro-Newton and nanometer range. Nanoindentation thus has become a powerful tool for probing the mechanical properties of materials at the micro- and nanometer length scale. It can be used also to simulate asperity contact over a wide range of length scales, which is very relevant to wear processes.

Our understanding of the theory of nanoindentation measurements has improved in recent years, both on the continuum level and to a lesser extent on the atomic level. For example, several methods have been proposed to obtain hardness, elastic moduli, initial yield strength and work-hardening exponent from nanoindentation measurements.<sup>50,51</sup> Similarly, the general shape of loading-unloading curves is now understood on the continuum level.<sup>52,53</sup> However, many questions remain, such as strain rate and temperature dependence and deformation mechanisms such as dislocation nucleation and movement that are not well described

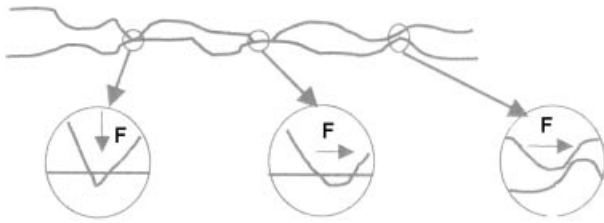


**Figure 2.** Three types of wear processes (left to right): indentation, plowing and asperity shear.

with continuum-level models. Similarly, even less is known about abrasive wear and how nanoscale contacts that involve plastic deformation are lubricated, such as that which occurs when a single tool asperity plows through the surface of a material in the presence of adsorbed additive molecules (see Fig. 2). Thus, there is a need for atomic-scale methods to investigate deformation phenomena and to try to link atomic-scale observations with macroscopic continuum models and experimental results.

During the last decade there has been a growing interest in the use of MD methods to investigate nanoindentation and wear. These methods can allow the simulation of up to millions of atoms for up to nanoseconds on current massively parallel architectures.<sup>54,55</sup> Several MD studies addressing some aspects of nanoindentation,<sup>56–68</sup> friction<sup>35,69–74</sup> and wear<sup>75,76</sup> have appeared already and more work is expected in the near future. Landman *et al.* carried out one of the first simulations of nanoindentations in which a nickel tip was indented into a gold substrate and they observed the formation of a connective neck at the tip-substrate interface<sup>56</sup> due to strong attractive bonding between the metals. Later they investigated the effect of a thin lubricant layer between metal asperities and observed that even a thin lubricant was enough to reduce greatly the adhesion and wear.<sup>57</sup> To study elastic contacts, Leng *et al.* investigated shallow nanoindentation (one or two atomic layers) with a series of room-temperature, constant-load MD simulations.<sup>58</sup> They found that the material's response was linear elastic during the loading–unloading cycle and the contact stresses were comparable with those calculated with macroscopic Hertzian theory. Buldum *et al.* used MD simulations to investigate the indentation, pull-out and dry sliding friction of a Ni tip on a relatively soft Cu surface, as well as the effects of the tip geometry (sharp or blunt).<sup>59</sup> They found that the load vs. indent depth curve displayed quasi-linear variations followed by a sudden decrease caused by disappearance of a layer. Similarly, Kelchner *et al.* modeled indentation of a Au(111) surface with a hard-sphere (non-atomic) indenter; their work provided atomistic imaging of dislocation nucleation during indentation on a 'passivated' surface.<sup>54</sup> Vashishta *et al.* briefly reported a single nanoindentation event of a 10 million atom Si<sub>3</sub>N<sub>4</sub> surface. Their simulations revealed significant plastic deformation and pressure-induced amorphization under the indenter and, from the loading–displacement curve, they estimated the hardness to be 50.3 GPa compared with the 21.6 GPa experimental value.<sup>55</sup> The amorphization and high hardness were due presumably to the high rate of their indentation (not reported). Ortiz and Phillips<sup>60,61</sup> have developed

a powerful hybrid approach that couples atomistic studies with continuum models, and they have applied it to the study of nanoindentation on large length scales. They investigated dislocation nucleation during indentation and found that increasing load dislocations nucleate at the indenter surface and propagate toward the crystal's interior, with steps in the loading curve similar to those found by Buldum. However, their method currently is limited to static calculations so they cannot study strain rate effects, temperature effects or the interplay between mechanical deformation and local heating.

In summary, several groups have begun to use MD to investigate nanoindentation. Several studies have been done and some interesting results have been reported. However, two of the studies involved only a single indentation event and one of the other studies only involved small elastic stresses. Several of the studies did not report fully their simulated conditions, such as strain rate or applied load. Most of the studies only investigated a single temperature for a single indentation rate, for a single-crystal orientation and for a single material combination. Thus, we felt that it was important to begin a systematic study to investigate, qualitatively and quantitatively, the many possible factors that can control nanoindentation and wear behavior.

There have been a few limited studies of wear processes at the atomic scale. For example, Landman *et al.* investigated the mechanism of adhesive contact formation, followed by sliding of the tip across the surface.<sup>75</sup> Similarly, Sorenson *et al.* did a few MD simulations of a small copper asperity (a few dozen atoms) bonding to another copper surface at room temperature, followed by shear.<sup>76</sup> However, there has not been any systematic theoretical investigation of the many factors that affect wear, such as temperature, load, velocity, orientation, tip–substrate interaction, asperity shape or alloy content. Thus, similar to our work on nanoindentation, we began a set of MD studies of wear that we discuss below.

### Recent MD simulations

We investigated several factors that determine the extent of indentation, including the effect of temperature, crystal orientation, tip shape, tip–substrate interaction and indent force/indent speed (details available from the author upon request). We chose aluminum as our model material because of our industrial partners and its widespread use in many industries, from aerospace to automotive to microelectronics. We described the atomic bonding with a simple embedded atom method potential that we had developed previously by fitting to a large DFT and experimental database.<sup>77</sup> It has proved to be surprisingly reliable for a wide range of relevant phenomena, including elastic deformation, phonons, thermal expansion, dislocation structure and melting, all of which can be involved in the plastic deformation that occurs during nanoindentation and wear. However, our results should be generic to most ductile fcc metals. Rather than specifying a specific indenter material, we chose to describe the indenter with a generic Lennard–Jones interaction, with the parameters chosen to represent a material much harder than Al because Al is a relatively soft metal that can be deformed easily by many other materials. Similarly, we chose to describe

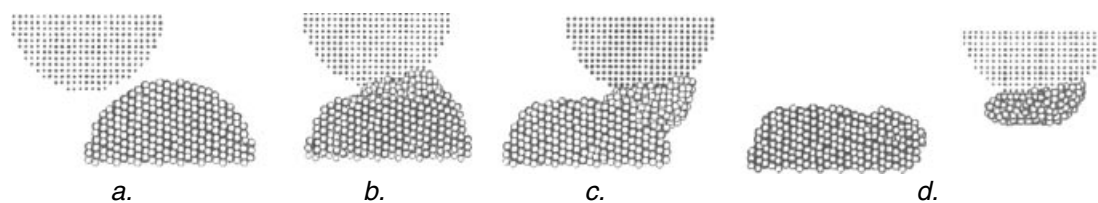


**Figure 3.** Molecular dynamics simulations of asperity plowing and adhesive metal transfer.

interactions between the Al and the indenter with a simple Lennard–Jones interaction, because that allows us to vary easily the bonding interactions and hence model the generic effects of a wide range of hard materials: from those that form passivated surfaces to those that form strong bonds with Al.

In conjunction with the Surface Tribology group at ALCOA and the Engineered Surfaces and Tribology group at General Motors, we carried out a wide range of simulations to determine the effect of several important parameters on the nature of loading/unloading nanoindentation curves and the atomic-scale mechanisms that controlled them. A typical nanoindenter simulation is shown in Plate 2. We investigated a variety of boundary conditions and found that they had little effect on our results provided that the indented region was small compared with the surrounding slab and provided that dislocations were free to move. Our simulations allowed us to determine how loading curves varied as a function of temperature, tip shape, crystal orientation and tip–substrate interaction. We found that rapid loading ( $>10 \text{ m s}^{-1}$ ) could result in local melting of the Al near the tip, with the disordered region increasing with increasing loading velocity. By taking advantage of the centrosymmetric crystal structure of Al, we were able to implement an algorithm to identify and track dislocations in the substrate, i.e. a centrosymmetric material will remain so under homogeneous elastic deformation but not under plastic deformation. We found that dislocations were emitted on multiple (111) planes in the [110] direction, as expected, and that approximately one dislocation loop formed for every layer indented. We found that the exact tip shape had little effect on the qualitative behavior, but the cross-sectional area in contact remained proportional to the remote stress (to maintain the local stress near the yield stress). We found that increasing the temperature from 0 K to 800 K (86% of the melting point) increased the indentation depth by 75%, corresponding to a decrease in the effective yield strength to 30% of its value at 0 K, which is roughly consistent with the temperature dependence of the bulk yield strength. We found that the loading curves were largely independent of the strength of the tip–substrate bonding interaction but that interaction had a large effect on the unloading curves, with high bond strengths resulting in the removal of more material and more plastic deformation. From the loading/unloading curves we were able to estimate the hardness of the Al to be 2MPa, which is reasonable for small indents into perfect single-crystal Al but high compared with the bulk. Most importantly, we found that the ordering of surface hardness was  $(110) < (111) < (100)$ , which was in qualitative agreement with the AFM tip (asperity) dragging results of our collaborators at ALCOA, who found the same ordering.<sup>78</sup>

In conclusion, we investigated many factors related to nanoindentation and determined their effect on loading/unloading curves. Several of our results are consistent with experimental observations, including the general shape of the loading/unloading curves, the temperature dependence and the surface orientation dependence. Most importantly, these atomic-scale simulations have helped to elucidate the deformation processes that can occur during nanoindentation.

In addition to our work on nanoindentation, we began a similar study to investigate how wear processes occur on the atomic level (details available from the author upon request). In general, when rough surfaces collide they can interact in many ways, as shown schematically in Fig. 2. These processes can be grouped loosely into the categories of indentation, plowing and asperity shear, with many wear events involving a combination of these aspects. Our recent modeling work has involved investigating many factors that affect asperity–asperity shear (details available from the author upon request). Figure 3 shows the sequence of a typical asperity shear process of Al. In general, our studies found that asperity shear at high speeds (e.g.  $100 \text{ m s}^{-1}$ ) resulted in local melting of the Al asperity, dislocation generation in the remnant Al surface along the favorable (111) planes and adhesive metal transfer of the Al onto the harder tool surface, even with very weak bonding between the Al and the tool. We varied the shear speed by an order of magnitude and found little change in the amount of material removed. We also varied the temperature and found that at 600 K the Al was significantly softer and more deformed. We are now investigating the effect of lower shear speeds, asperity geometry, the degree of overlap and tip–Al bonding. Overall, we find that the degree of overlap is the most important factor in determining the amount of material removed (wear rate), but that other factors (tip–Al bonding and temperature) can significantly affect the amount of wear and the amount of plastic deformation in the remaining Al. The power of this approach is that we can easily quantify the wear removal rate (number of atoms removed) and the amount of plastic deformation (change in the system's potential energy). We are now working on developing an analytical expression that can predict the amount of wear based on our simulation variables.

## CONCLUSION

In conclusion, there has been great recent interest in increasing our understanding of adhesion, lubrication and wear on the atomic scale. Some interesting work has been done and we think that there is a lot more still to do. We

believe that an atomic-scale understanding of these complex phenomena will allow us to better engineer the products so that we can produce them more efficiently and increase their performance and durability.

### Acknowledgements

J.B.A, D.S., H.Y. and J.Z. acknowledge support from the National Science Foundation under grant number DMR 9619353 and computational support on the SGI machines at NCSA. D.S. and H.Y. acknowledge summer support from General Motors.

### REFERENCES

- Finnis MW. *J. Phys.: Condens. Matter*. 1996; **8**: 5811.
- Humenik M, Kingery WD. *J. Am. Ceram. Soc.* 1954; **37**: 18.
- Howe JM. *Int. Mater. Rev.* 1993; **38**: 233.
- McDonald JE, Eberhart JG. *Trans. Metall. Soc. AIME* 1965; **233**: 512.
- Barrera RG, Duke CB. *Phys. Rev. B* 1976; **13**: 4477.
- Laurent V, Chatain D, Chatillon C, Eustathopoulos N. *Acta Metall.* 1988; **36**: 1797.
- Chatain D, Coudurier L, Eustathopoulos N. *Rev. Phys. Appl.* 1988; **23**: 1055.
- Eustathopoulos N, Chatain D, Coudurier L. *Mater. Sci. Eng.* 1991; **A135**: 83.
- Hohenberg P, Kohn W. *Phys. Rev.* 1964; **136**: 864B.
- Kohn W, Sham LJ. *Phys. Rev.* 1965; **140**: 1133A.
- Kohyama M. *J. Mode. Simul. Mater. Sci. Eng.* 1996; **4**: 397.
- Hoekstra J, Kohyama J. *Phys. Rev. B* 1998; **57**: 2334.
- Kohyama M, Hoekstra J. *Phys. Rev. B* 2000; **61**: 2672.
- Benedek R, Minkoff M, Yang LH. *Phys. Rev. B* 1996; **54**: 7697.
- Batirev IG, Alavi A, Finnis MW. *Phys. Rev. Lett.* 1999; **82**: 1510.
- Rao F, Wu R, Freeman AJ. *Phys. Rev. B* 1995; **51**: 10052.
- Kostlmeier S, Asser CE, Meyer B, Finnis MW. *Mater. Res. Soc. Proc.* 1998; **492**: 97.
- Dudiy SV, Hartford J, Lundqvist BI. *Phys. Rev. Lett.* 2000; **85**: 1898.
- Hartford J. *Phys. Rev. B* 2000; **61**: 2221.
- Ogata S, Kitagawa H. *J. Jpn. Inst. Met.* 1996; **60**: 1079.
- Benedek R, Alavi A, Seidman DN, Yang LH, Muller DA, Woodward C. *Phys. Rev. Lett.* 2000; **84**: 3362.
- Zhukovskii YF, Kotomin EA, Jacobs PWM, Stoneham AM. *Phys. Rev. Lett.* 2000; **84**: 1256.
- Zhang W, Smith JR. *Phys. Rev. Lett.* 1999; **82**: 3105.
- Benedek R, Seidman DN, Minkoff M, Yang LH, Alavi A. *Phys. Rev. B* 1999; **60**: 16094.
- Zhang W, Smith JR. *Phys. Rev. B* 2000; **61**: 16883.
- Kresse G, Furthmüller J. *Phys. Rev. B* 1996; **54**: 11169.
- Siegel DJ, Hector Jr LG, Adams JB. *Phys. Rev. B* (submitted).
- Hellmann H. *Einführung in die Quantumchemie*. Deuticke: Leipzig, 1937.
- Lipkin DM, Clarke DR. *Philos. Mag. A* 1997; **76**: 715.
- Savin A, Nesper R, Wengert S, Fassler TF. *Angew. Chem. Int. Ed. Engl.* 1997; **36**: 1808.
- Mayer I. *Chem. Phys. Lett.* 1983; **97**: 270.
- Mulliken RS. *J. Chem. Phys.* 1955; **23**: 1833, 2343.
- Israelachvili JN, McGuiggan PM, Homola AM. *Science* 1988; **240**: 189–191.
- Alsten VJ, Granick S. *Phys. Rev. Lett.* 1988; **61**: 2570.
- Harrison JA, Stuart SJ, Brenner DW. *Handbook of Micro/Nanotribology*. Bhushan B (ed.). CRC Press: Boca Raton, 1999; 525–594.
- Jiang S, Frazier R, Yamaguchi ES, Blanco M, Dasgupta S, Zhou Y, Cagin T, Tang Y, Goddard III WA. *J. Phys. Chem. B* 1997; **101**: 7702.
- Cagin T, Zhou Y, Yamaguchi ES, Frazier R, Ho A, Tang Y, Goddard III WA. *Mater. Res. Soc. Symp. Proc.* 1999; **543**: 79.
- Zhou Y, Jiang S, Cagin T, Yamaguchi ES, Frazier R, Ho A, Tang Y, Goddard III WA. *J. Phys. Chem. A* 2000; **104**: 2508.
- John A. Schey. *Tribology in metalworking: friction, lubrication, and wear*, American Society for Metals: Metals Park, OH, 1983.
- Rogers JW, Hance RL, White JM. *Surf. Sci.* 1980; **100**: 388.
- Reich RA, Mendoza E. *J. Soc. Tribol. Lub. Eng. Lubr. Eng.* 1997; **54**: 10.
- Laemmle JT. *J. Soc. Tribol. Lubr. Eng. Lubr. Eng.* 1986; **43**: 717.
- Hooper A, Fisher GL, Jung D, Nguyen H, Opila R, Collins RW, Winograd N, Allara DL. *J. Am. Chem. Soc.* 1999; **121**: 8052.
- Underhill R, Timsit RS. *J. Vac. Sci. Technol. A* 1992; **10**: 2767.
- Opalka SM, Hector Jr LG, Schmid S, Reich RA, Epp JM. *ASME: J. Tribol.* 1998; **121**: 384.
- Hector Jr LG, Nitowski GA, Opalka SM, Wieserman L, Siegel D, Yu H, Adams J. *Phys. Rev. B* (submitted).
- Nitowski GA. *PhD Thesis*, Virginia Polytechnic State University, 1998.
- Coast R, Pikus M, Henriksen PN, Nitowski GA. *J. Adhes. Sci.* 1996; **2**: 101.
- Likhtman VI, Rebinder PA, Karpenko GV. *Effect of Surface-Active Media on the Deformation of Metals*. Chemical Publishing Company: New York, 1960.
- Oliver W, Pharr G. *J. Mater. Res.* 1992; **7**: 1564.
- Cheng YT, Cheng CM. *Appl. Phys. Lett.* 1998; **73**: 614.
- Cheng YT, Cheng CM. *J. Appl. Phys.* 1998; **84**: 1284.
- Cheng YT, Cheng CM. *J. Mater. Res.* 1999; **14**: 3493.
- Kelchner CL, Plimpton SJ, Hamilton JC. *Phys. Rev. B* 1998; **58**: 11085.
- Vashishta P, Bachlechner ME, Campbell T. *Prog. Theo. Phys. Suppl.* 2000; **138**: 175.
- Landman U, Luedtke WD, Burnham N, Colton R. *Science* 1990; **248**: 454.
- Gao J, Luedtke WD, Landman U. *Science* 1995; **270**: 605.
- Leng Y, Yang G, Hu Y, Zheng L. *J. Mater. Sci.* 2000; **35**: 2061.
- Buldum A, Ciraci B, Batra IP. *Phys. Rev. B* 1998; **57**: 2468.
- Ortiz M, Phillips R. *Adv. Appl. Mech.* 1999; **36**: 1.
- Phillips R, Rodney D, Sheney V, Tadmor E, Ortiz M. *J. Model. Simul. Mater. Sci. Eng.* 1999; **7**: 769.
- Komvopoulos K, Yan W. *J. Appl. Phys.* 1997; **82**: 4823.
- Rafii-Tabar H, Kawazoe Y. *J. Appl. Phys.* 1993; **32**: 1394.
- Pokropiny VV, Skorokhod VV. *J. Model. Simul. Mater. Sci. Eng.* 1997; **5**: 579.
- Zhang LC, Tanaka H. *JSME Int.* 1999; **42**: 546.
- Astala R, Kaukonen M. *Phys. Rev. B* 2000; **61**: 2973.
- Belak, Stowers I. *Fundamentals of Friction: Macroscopic and Microscopic Processes*. Singer LL, Pollock HM (eds). Klumer Academic Boston, 1992; 511–520.
- Tomagnini O, Ercolessi F, Tosatti E. *Surf. Sci.* 1993; **287**: 1041.
- Zhang L, Tanaka H. *Wear* 1997; **211**: 44.
- Komanduri R, Chandrasekaran N, Raff L. *Phys. Rev. B* 2000; **61**: 14007.
- Persson BN. *Phys. Rev. Lett.* 1993; **71**: 1212.
- Harrison JA, White CT, Colton RJ, Brenner DW. *Phys. Rev. B* 1992; **46**: 9700.
- McClelland GM, Cohen SR. *J. Apply. Phys.* 1993; **73**.
- Fukuyama H, Matsukawa H. *Phys. Rev. B* 1994; **49**: 17286.
- Landman U, Luedtke WD, Ringer Eric M. *Wear* 1992; **153**: 3.
- Sorensen MR, Jacobson KW, Stoltze P. *Phys. Rev. B* 1996; **53**: 2101.
- Ercolessi F, Adams JB. *Europhys. Lett.* 1994; **26**: 583.
- Hector Jr LG, Opalka SM, Weiland H, Schmid SR. In *Fundamentals of Nanotribology*, MRS Symposium Proceeding 1998 Vol. 522 pp. 399–408.